Longitudinal and transverse dispersion coefficients in braided rivers

Li Gu, Zinan Jiao and Zulin Hua

ABSTRACT

The dispersion characteristics of braided rivers are presently unclear. The comprehensive flow structure in a physical braided river model was measured and was used to estimate its dispersion coefficient tensor. The largest values of the longitudinal and transverse dispersion coefficients occurred in the separation zone in two anabranches. The separation zone disappeared in a small diversion angle model of braided rivers where the coefficients were smaller. As for the sectional transverse distribution, the two coefficients varied markedly and an interesting negative correlation between them appeared in several sections. The dispersion coefficients increased with upstream flow rates. Comparison between the coefficients for different anabranch widths revealed higher values in wider sections. Finally, the values of the laboratory tests were compared with those in a real braided river, and relatively larger coefficients were found in natural rivers. The findings of this paper could be helpful in understanding the dispersion characteristics and in estimating pollutant concentration in braided rivers.

Key words | braided river, dispersion coefficients, secondary flow, separation zone, vertical velocity distribution

Li Gu
Zinan Jiao
Zulin Hua (corresponding author)
Key Laboratory of Integrated Regulation and Resource Development on Shallow Lake of Ministry of Education,
College of Environment,
Hohai University,
Nanjing 210098,
China
E-mail: *zulinhua@hhu.edu.cn*

Li Gu
Zulin Hua
National Engineering Research Center of Water Resources Efficient Utilization and Engineering Safety,
Hohai University,
Nanjing 210098,
China

INTRODUCTION

The dispersion coefficient is an important parameter representing dispersion characteristics of a river, and plays a great role in estimating pollutant concentration successfully. Substantial efforts have been made by Fischer *et al.* in the past few decades to estimate longitudinal and transverse dispersion coefficients in a regular straight channel. The dimensionless transverse mixing coefficient in rectangular channels varied from 0.1 to 0.2 (Fischer *et al.* 1979). The value was 0.17 in a straight section of the river Rhine near Karlsruhe measured by Webel & Schatzmann (1984). As to the dimensionless longitudinal dispersion coefficient, its value was equal to 5.93 for a vertical logarithmic velocity profile in an infinitely wide channel (Elder 1959). In general, the coefficient in natural straight rivers was much greater than Elder's result. Seo & Cheong (1998) pointed out that the coefficient was 395.11 in the Mississippi River. Greater longitudinal dispersion coefficients were also estimated by Yotsukura *et al.* (1970) and Fuat Toprak & Savci (2007).

Based on the research of regular straight channels, the effects of more factors such as bed roughness, cross-sectional shape, curvature, and vegetation in natural channels on dispersion were taken into account (Fukuoka & Sayre 1973; Hou & Christensen 1976; Deng *et al.* 2001; Perucca *et al.* 2009). High bed surface roughness was found to increase the gradient in vertical velocity profiles and, thus, shear dispersion (Schulz *et al.* 2012). An empirical formula considering the radius of curvature and overall bend length was proposed by Fukuoka & Sayre (1973) for meandering rivers. In the river with riparian vegetation, a quite sparse riparian vegetation can affect longitudinal dispersion by 70–100% with respect to the case without vegetation (Perucca *et al.* 2009).

However, the dispersion coefficients may not be homogeneous along the natural river because of the heterogeneous flow characteristics (Piasecki & Katopodes 1999). The space variation of dispersion coefficients has been observed in the meandering channel. Sayre & Yeh (1973) reported that in a meandering channel transverse mixing coefficients vary from one-half its average value in the upstream portion of a bend to twice the average in the downstream portion. In sinuous open channels, the maximum transverse dispersion coefficients are reached

doi: 10.2166/wst.2014.212

downstream of the bend apex in the regions of strong secondary flow, and minimum values in the straighter regions (Boxall & Guymer 2003). A similar phenomenon was also reported in the North Saskatchewan River (Dow *et al.* 2009). Furthermore, in the section of the meander cycle running from apex to cross-over, longitudinal dispersion coefficients were lower than the apex to apex values, whist the cross-over to apex reach had higher values (Boxall & Guymer 2007).

Spatial variation of dispersion coefficient in meandering channels is mainly caused by their complicated flow structure, and especially for the transverse dispersion the secondary currents play a great role. Compared with meandering channels, the braided river has more complex morphology and flow dynamics (Richardson *et al.* 1996), and thus its dispersion characteristics will have an obvious spatially heterogeneous distribution, which is more attractive to researchers. However, few studies on dispersion in braided rivers have been reported so far, and their dispersion characteristics are unclear, especially the spatial distribution of longitudinal and transverse dispersion coefficients.

The present paper extends the previous work on dispersion to the braided river, and detailed information of spatial distribution of dispersion coefficients in braided rivers was first analyzed. Laboratory tests in the braided river model were conducted, and the components of the dispersion tensor were calculated using velocity profiles. Dispersion characteristics for various flow rates, different anabranch widths, and different diversion angles were compared. The relationships between dispersion properties and cross-sectional secondary flow were further analyzed. Moreover, the influence of a separation zone is also discussed. Finally, the dispersion coefficients in the anabranch of the braided Brahmaputra River were calculated, and the relevance of the laboratory to the natural braided river are discussed.

MATHEMATICAL METHOD

Following the definition of the one-dimensional longitudinal dispersion coefficient, the equation for the dispersion tensor was given by Fischer (1978):

$$\dot{M}_x = -h\left(D_{xx}\frac{\partial\langle c\rangle}{\partial x} + D_{xy}\frac{\partial\langle c\rangle}{\partial y}\right) \tag{1a}$$

$$\dot{M}_y = -h\left(D_{yx}\frac{\partial\langle c\rangle}{\partial x} + D_{yy}\frac{\partial\langle c\rangle}{\partial y}\right) \tag{1b}$$

Then the Cartesian components of the dispersion tensor are given:

$$D_{xx} = -\frac{1}{h}\int_o^h u'\int_0^z \frac{1}{\varepsilon}\int_o^z u'\,dz\,dz\,dz \tag{2a}$$

$$D_{xy} = -\frac{1}{h}\int_o^h u'\int_0^z \frac{1}{\varepsilon}\int_o^z v'\,dz\,dz\,dz \tag{2b}$$

$$D_{yx} = -\frac{1}{h}\int_o^h v'\int_0^z \frac{1}{\varepsilon}\int_o^z u'\,dz\,dz\,dz \tag{2c}$$

$$D_{yy} = -\frac{1}{h}\int_o^h v'\int_0^z \frac{1}{\varepsilon}\int_o^z v'\,dz\,dz\,dz \tag{2d}$$

where M_x and M_y denote unit width mass flux in x and y direction, $<c>$ is the depth average of c, $h =$ the local depth of flow, u' and v' denote vertical deviations of point velocities with respect to depth-averaged velocities u and v respectively, z is the vertical coordinate, and ε is a vertical turbulent diffusion coefficient. Therefore, measured velocity data can be used to calculate the Cartesian components of the dispersion tensor.

The longitudinal and transverse dispersion coefficients along the streamline and normal to the streamline are defined as D_{L} and D_{T}. The Cartesian components of the dispersion coefficient tensor (D_{xx}, D_{xy}, D_{yx}, D_{yy}) are related to D_{L} and D_{T} (Alavian 1986):

$$D_{xx} = D_L\frac{u^2}{U^2} + D_T\frac{v^2}{U^2} \tag{3a}$$

$$D_{xy} = D_{yx} = (D_L - D_T)\frac{uv}{U^2} \tag{3b}$$

$$D_{yy} = D_T\frac{u^2}{U^2} + D_L\frac{v^2}{U^2} \tag{3c}$$

By relating Equation (2) to Equation (3), the longitudinal and transverse dispersion coefficients D_{L} and D_{T} can be estimated from the calculated components of the dispersion coefficient tensor. The calculated values of D_{xy} and D_{yx} obtained using vertical profile data have almost the same values, and therefore these two terms are averaged to be

used in Equation (4) (Seo *et al.* 2008):

$$\begin{pmatrix} D_L \\ D_T \end{pmatrix} = (A^T A)^{-1} A^T \begin{pmatrix} D_{xx} \\ D_{yx} = D_{xy} \\ D_{yy} \end{pmatrix} \tag{4}$$

where

$$A = \begin{bmatrix} \dfrac{u^2}{U^2} & \dfrac{v^2}{U^2} \\ \dfrac{uv}{U^2} & -\dfrac{uv}{U^2} \\ \dfrac{v^2}{U^2} & \dfrac{u^2}{U^2} \end{bmatrix}$$

is a matrix and $U = \sqrt{u^2 + v^2}$.

The bicubic interpolation method is used to calculate the values of the dispersion coefficient tensor. The velocity profile within the boundary layer changes dramatically, while the accuracy of measured velocities 0.5 cm from the bottom can be confirmable. The velocity profile was assumed to be decreased linearly to zero at the bottom of channel for simplicity. Thus, relative results can be obtained by numerical integration of Equation (2).

EXPERIMENTS

To study dispersion properties along anabranches, a laboratory physical model of the braided river was constructed. The flume was made of organic glass and was 25 m long. The width of the upstream main channel, left anabranch and right anabranch were denoted as B_0, B_1, and B_2, respectively (Figure 1(a)). The parameter $B^*(B^* = B_1/(B_1 + B_2))$, which was the ratio of the width of the left anabranch to the sum widths of the two anabranches, was introduced. B_0 was equal to 0.5 m, and $B_1 + B_2 = 0.7$ m. The mid-bar could be moved to change the width of the two anabranches. The inner bank was defined as the wall close to the mid-bar and the outer bank was located on the other side. Different width ratios of the two anabranches and different upstream flow rates were considered in the experiments, as listed in Table 1.

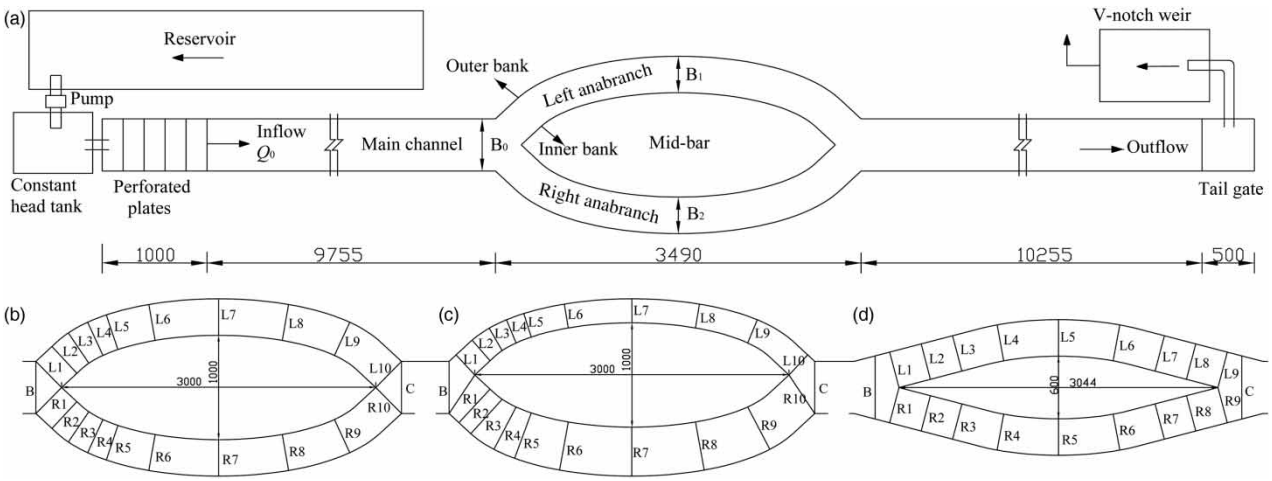

Figure 1 | Diagram of the experimental model (a), and location diagrams of measured sections with (b) case 1 with $B^* = 0.5$, (c) case 3 with $B^* = 0.33$ and (d) case 4 with $B^* = 0.5$ (length unit: mm).

Table 1 | Experimental flow conditions

Case	Diversion angle (θ)	B^*	Discharge of inflow Q_o (L/s)	Flow depth H_o (m)
1	86°	0.5	5.96 (Run F-1), 7.51 (Run F-2), 9.69 (Run F-3), 11.18 (Run F-4), 13.41 (Run F-5)	0.149
2	86°	0.41	7.51	0.149
3	86°	0.33	7.51	0.149
4	29°	0.50	8.04	0.139

In addition, two diversion angles were used to investigate the effect of the separation zone on the dispersion.

The velocity data were measured by a three-component Sontek ADV. Ten sections were set up in each anabranch for cases 1 to 3, and nine sections were used in case 4 (Figures 1(b)–1(d)). For convenience of analysis in the following experiments, S1, S2, …, S10 were assigned as the names of sections in the anabranch, whether in the left or the right anabranch. In each cross-section, seven to nine verticals were measured, with six to eight test points along each vertical. The position of verticals for measuring velocity are shown in Table 2.

ESTIMATION OF DISPERSION COEFFICIENTS IN ANABRANCHES

The dimensionless values of D_L/hu^* and D_T/hu^* were calculated and analyzed in the braided river models with different width ratios, upstream flow rates and diversion angles. Shear velocity is estimated by the following equation $u^* = (gRS_f)^{1/2}$, where g is the acceleration of gravity; R is the hydraulic radius; $S_f = n^2U^2R^{-4/3}$ is the friction slope; and n is Manning coefficient. In the analysis of the longitudinal variation along the anabranch, the section-averaged D_L and D_T were used.

Dispersion in anabranches with the separation zone

Contours for the longitudinal and transverse dispersion coefficients in case 1 are shown in Figures 2(a) and 2(b) respectively. It is obvious that D_L/hu^* and D_T/hu^* both have relatively large values near the outer bank in the first half of the anabranch where the separation zone occurs. Higher values of D_T/hu^* also appear near the inner bank, which has relatively high values of stream-wise velocity in the first few sections. In the second half of the anabranches, from section S7 to S10, dispersion coefficients become smaller and vary less. The velocity fields at the surface and the bottom for case 1 are depicted in Figures 2(e) and 2(f) respectively. It is apparent that the velocity varies widely between the bottom and the surface in the separation zone, which contributes to larger values of the dispersion coefficients. This increase is consistent with the features observed in the stream with the 'dead zones' (Valentine & Wood 1977). Velocity differences between the bottom and the surface were small in the second half of the anabranches, leading to relatively smaller coefficient values. Section L7 and L9 were chosen to investigate the influence of secondary flow on the transverse dispersion coefficients. In section L7 of case 1, the variations of D_L/hu^* and D_T/hu^* exhibited a similar pattern in the transverse direction (Figure 2(i)). The reason was that the center of the secondary flow cell in section 7 had a stronger velocity deviation and its location was close to the main stream-wise flow. Thus a similar one-peak distribution of D_L/hu^* and D_T/hu^* was caused. An interesting negative correlation was found in section L9 (Figure 2(j)). It is clear that there are two cells of secondary flow with opposite directions of rotation in this section (Figure 2(h)). Each of the cells is skewed to one side wall, leading to two peaks of D_T/hu^*, and the main flow is located in the center of the cross-section which is between two cells. All these factors contribute to the negative correlation of D_L/hu^* and D_T/hu^*.

The longitudinal variation of the section-averaged dispersion coefficients in case 1 is shown in Figures 2(c) and 2(d). Due to the symmetrical arrangement of the two anabranches, the left anabranch was chosen for detailed analysis. D_L/hu^* and D_T/hu^* had similar variation trends along the anabranch. They both exhibited the unimodal distribution pattern, with the highest value occurring in section L3. The values of D_L/hu^* varied between 2.17 and 7.79 in sections S1 to S6 and between 0.4 and 1.5 in sections S7 to S10. Figure 2(e) shows that a separation zone appeared from S2 to S5, which dramatically enhanced the dispersion ability. Therefore, the average values of D_T/hu^* also

Table 2 | Position of verticals for measuring velocity

			Distance from the outer bank (cm)	
Case	**Number of verticals (anabranch-1)**	**Number of verticals (anabranch-2)**	**Position of verticals (anabranch-1)**	**Position of verticals (anabranch-2)**
1	7	7	5, 9, 13, 17.5, 22, 26, 30	5, 9, 13, 17.5, 22, 26, 30
2	6	8	4.5, 8.5, 12.5, 16.5, 20.5, 24.5	5, 9.5, 14, 18.5, 22.5, 27, 31.5, 36
3	5	9	4.5, 8, 12, 16, 19.5	5, 9.5, 14, 18.5, 23, 27.5, 32, 36.5, 41
4	7	7	5, 9, 13, 17.5, 22, 26, 30	5, 9, 13, 17.5, 22, 26, 30

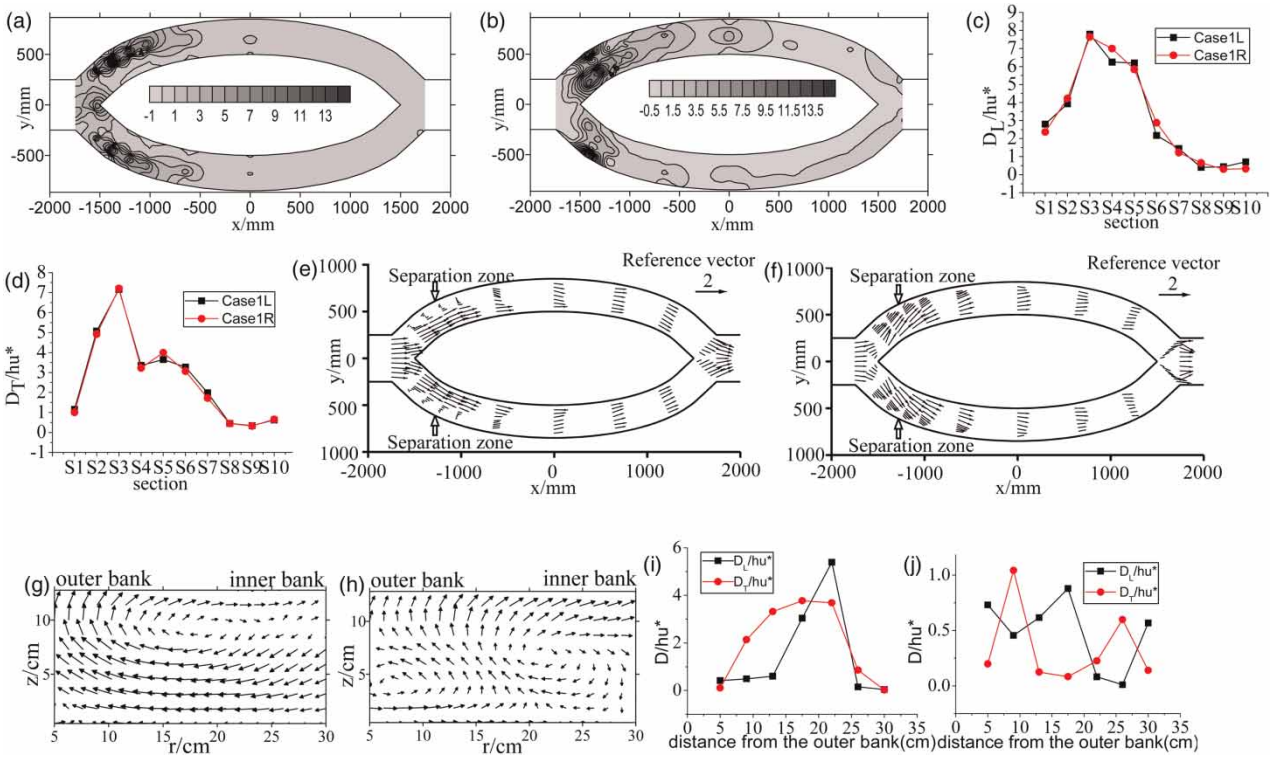

Figure 2 | Distributions of D_L/hu^* and D_T/hu^* and the flow structure in case 1: (a) contour of D_L/hu^*, (b) contour of D_T/hu^*, (c) section-averaged D_L/hu^*, (d) section-averaged D_T/hu^*, (e) flow field at the surface ($z = 12.7$ cm), (f) flow field at the bottom ($z = 0.5$ cm), (g) and (h) secondary flow in L7 and L9, (i) and (j) transverse variation in L7 and L9.

increased in the first half of the anabranch, ranging from 1.16 to 7.16. The average value of D_T/hu^* for sections far from the separation zone, including sections S8, S9, and S10, varied from 0.34 to 0.62, which is comparable to the results of Holley & Abraham (1973) for a curved channel. Rutherford (1994) also reported that D_T/hu^* varied from 0.3 to 0.9 in meandering natural channels and ranged from 1 to 3 in curved channels with a strong secondary flow. In the lower half of the anabranch, the results of a braided river were similar to the values for natural curved channels.

Contours for dispersion coefficients in cases 2 and 3 are shown in Figures 3(a)–3(d). Obviously, the existence of the separation zone still led to larger values of dispersion coefficients in the first half of the anabranches. Compared with case 2, the zone of high dispersion coefficients in case 3 was larger. The reason for this was that larger separation-zone areas and higher velocity magnitudes existed in the wider right anabranch of case 3. In case 1, with $B^* = 0.5$, the dispersion coefficients did not change in the confluence. However, in cases 2 and 3, with two asymmetric anabranches, the dispersions were obviously enhanced in the confluence. There was a negative correlation between dispersion in the confluence and the width ratio B^*. The non-uniform velocity distribution caused by the flow mixing from two asymmetric anabranches with different flow rates might have been the reason for this. A few interesting negative values can be found in the separation zone, which were caused by measured negative velocity values. This is a unique phenomenon which can be found only in the separation zone.

In cases 2 and 3, the variations of section-averaged D_L/hu^* and D_T/hu^* in the left and right anabranches are shown in Figures 3(e)–3(h). It can be concluded that the values of D_L/hu^* and D_T/hu^* generally increased with increasing anabranch width, and that longitudinal variation had a similar trend to case 1, which means that the highest value appeared in the sections in the separation zone in all cases. The value of D_T/hu^* varied from 0.26 to 5.5 for the left anabranch and from 0.41 to 7.10 for the right anabranch in case 2 (from section S1 to S10). In case 3, D_T/hu^* ranged from 0.19 to 3.07 in the left anabranch and from 0.77 to 7.64 in the right anabranch (from section S1 to S10).

Furthermore, the dispersion coefficients in the five cases with different flow rates ((Run F-1 to Run F-5, in Table 1) were calculated. In the left anabranch, both D_L and D_T increased as the flow rate Q increased. The results for the

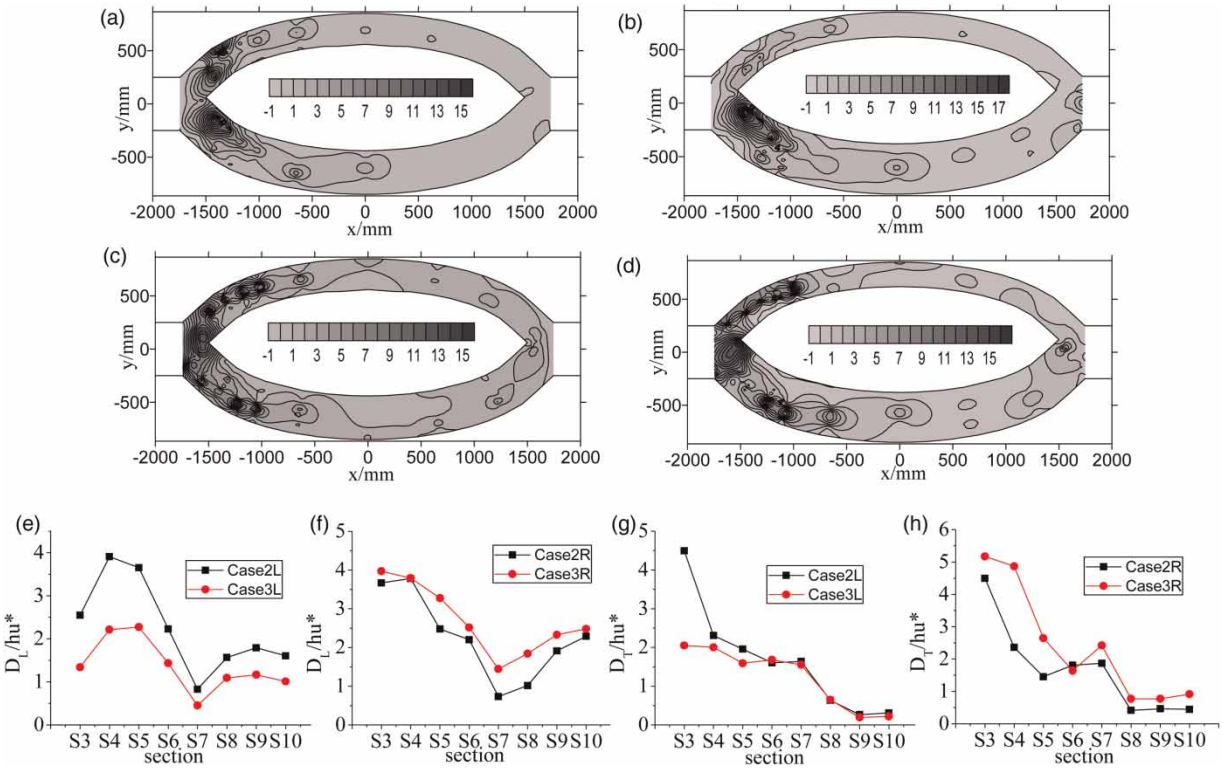

Figure 3 | D_L/hu^* and D_T/hu^* in cases 2 and 3: (a) and (b) contour of D_L/hu^* in case 2 and 3, (c) and (d) contour of D_T/hu^* in cases 2 and 3, (e) and (f) section-averaged D_L/hu^* of the left and right anabranch, (g) and (h) section-averaged D_T/hu^* of the left and right anabranch.

experimental data in braided rivers are consistent with earlier studies in single rivers (Elder 1959; Fischer *et al.* 1979).

Dispersion in anabranches without a separation zone

Contours for dispersion coefficients in case 4 without a separation zone are depicted in Figures 4(a) and 4(b). Higher values were found in the entrance and exit of the anabranches, which was different from rivers with a separation zone. The minimum value appeared near the apex of each anabranch. Compared with case 1, the dispersion coefficients were relatively smaller in case 4. Whether or not the separation zone existed, higher values could also be found at the head of the mid-bar. This

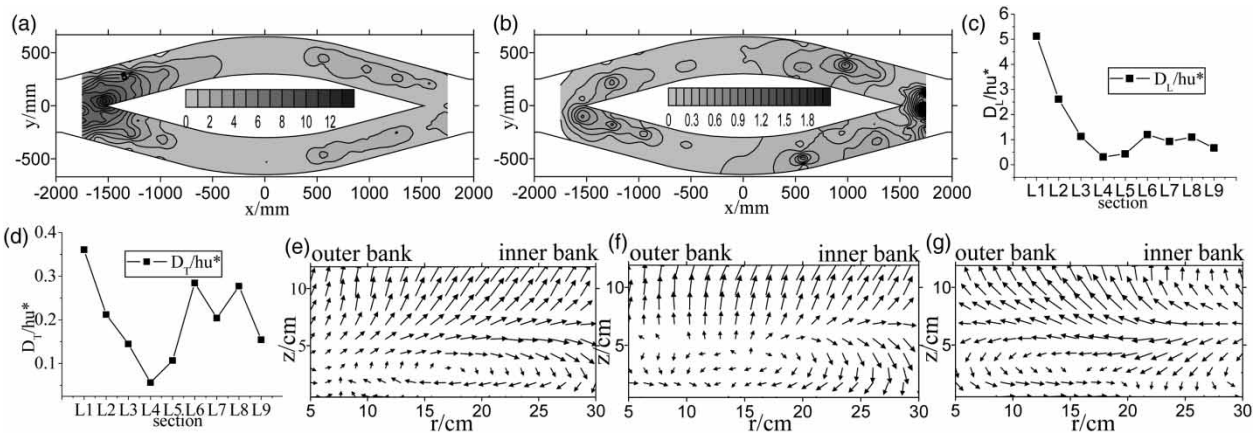

Figure 4 | D_L/hu^* and D_T/hu^* and flow structure in case 4: (a) contour of D_L/hu^*, (b) contour of D_T/hu^*, (c) longitudinal variation of section-averaged D_L/hu^*, (d) longitudinal variation of section-averaged D_T/hu^*, (e)–(g) secondary current in L2, L4, and L7.

occurred because a relatively lower velocity value appeared at the bottom of the inner bank near the head of the mid-bar, leading to a stronger velocity deviation.

The longitudinal variation of the dimensionless section-averaged dispersion coefficients is also shown in Figures 4(c) and 4(d) and has a different trend from case 1. The highest value of D_L/hu^* (5.12) was found in the entrance of the anabranch, and the value decreased along the anabranch until section L4, after which the value was basically stable. The highest value of D_L/hu^* (7.79) in case 1 was almost 1.5 times the highest value (5.12) in case 4.

The minimum value of D_T/hu^* (0.06) occurred in section L4 (Figure 4(d)). As shown in Figures 4(e)–4(g), it is interesting to note that the helical direction of the secondary flow was reversed after section L4. The magnitude of the transverse velocities was relatively smaller here. Therefore, the dimensionless value of D_T/hu^* in section L4 was smallest. However, the existence of one secondary flow cell in sections L2 and L7 led to a higher value of D_T/hu^*. The value of D_T/hu^* in case 4 varied from 0.06 to 0.36, which was smaller than the value in case 1. The results for a braided river with small diversion angle were similar to these values, ranging from 0.09 to 0.24 in the laboratory rectangular channel investigated by Okoye (1970). It can be concluded that the values of D_L/hu^* and D_T/hu^* decrease as the diversion angle decreases.

The transverse variation of the dispersion coefficients in the separation zone of case 1 was compared with that in case 4. As shown in Figure 5, section L3 was chosen for comparison. The value of D_L/hu^* was much higher near the outer bank, where a separation zone occurred, but its value decreased quickly outside the separation zone in section L3. An obvious negative correlation between D_L/hu^* and D_T/hu^* can be seen in section L3 for case 1. By comparison, the values of D_L/hu^* and D_T/hu^* in case 4 were smaller and varied little over the section where there is no separation zone.

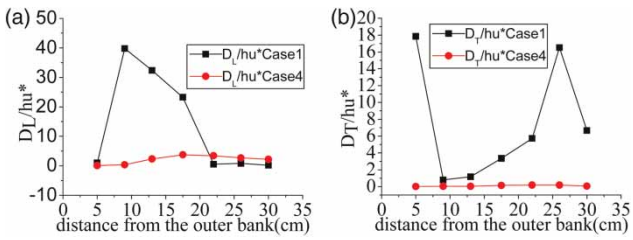

Figure 5 | Transverse variation of D/hu^* in section L3 for cases 4 and 1: (a) D_L/hu^*, (b) D_T/hu^*.

Correlation between longitudinal and transverse dispersion

In the low range of the transverse dispersion coefficient, an exponential increase in the longitudinal dispersion coefficient was found by Boxall & Guymer (2007) as the transverse dispersion coefficient decreased. In the anabranch of braided rivers, there was no obvious relationship in the separation zone, where both D_L/hu^* and D_T/hu^* were extremely large. However, in the lower half of the anabranch without a separation zone, an obvious negative correlation between the distributions of longitudinal and transverse dispersion coefficients existed (Figure 6), where the longitudinal dispersion coefficient was increasing when the transverse dispersion coefficient was decreasing.

DISCUSSION

In order to reveal the correlation between the values obtained in laboratory experiments and a natural river, dispersion in a braided channel of the Brahmaputra River in Bangladesh is discussed further. Velocity profile in the anabranch was measured by Richardson *et al.* (1996), and its dispersion coefficients were calculated by using Equation (4). The transverse variation of D_L/hu^* and D_T/hu^* at the entrance section of the left anabranch (May 1994 survey) are presented in Figure 7. The maximum value of

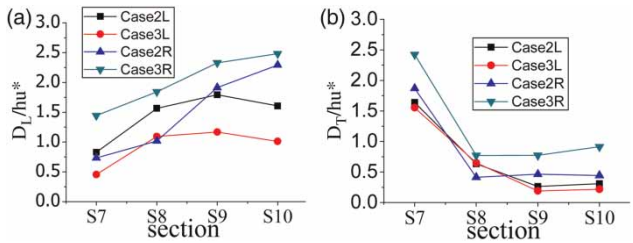

Figure 6 | Dispersion coefficients in cases 2 and 3 (S7-S10): (a) D_L/hu^*, (b) D_T/hu^*.

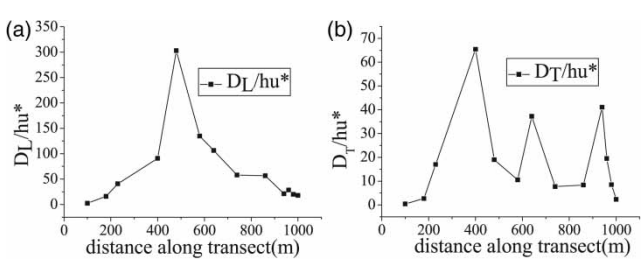

Figure 7 | Transverse variation of dimensionless dispersion coefficients D/hu^*.

D_L/hu^* happened above the talweg where the primary isovels displayed a single core of maximum velocity (Figure 7(a)). Compared with the entrance section 3 in case 1 with a large diversion angle, a roughly similar transverse variation could be found (Figure 5(a)). Its maximum value of D_L/hu^* also occurs at the location of the primary flow. According to the analysis of Richardson *et al.* (1996), strong secondary flow was found on the left side of the channel (250 m to 600 m) and in the right side of the channel (850 m to 1044 m). Thus higher dispersion coefficients were observed at the two places and two peak values could be seen in Figure 7(b). The same conclusion was drawn before in the laboratory tests and the Figure 5(b) shows two similar peaks of D_T/hu^* in two sides of the channel for case 1. Differently, Figure 7(b) shows a third peak of higher values between 600 to 700 m where there is a biggest flow depth. In general, higher magnitude of values was found in real rivers. D_L/hu^* varies from 2.35 to 302.74 and D_T/hu^* varies from 0.45 to 65.41. This is mainly because of the higher speed in the natural rivers compared with that in the laboratory channel. Furthermore, an irregular section shape and bed surface roughness are also responsible for this in natural rivers.

CONCLUSIONS

Experimental vertical profiles of longitudinal and transverse velocities were used to estimate dispersion coefficients along the anabranch in braided rivers. The results showed that the existence of a separation zone dramatically enhanced the dispersion ability. Both D_L and D_T increased with the increasing flow rate. As the width of the anabranch became larger, the dispersion coefficients increased as well. Moreover, the value of the longitudinal and transverse dispersion coefficients in case 4 without a separation zone was smaller than that in cases with a separation zone. There was an obvious negative correlation between the distributions of longitudinal and transverse dispersion coefficients in the lower half of the anabranch, far away from the separation zone. An interesting transverse negative correlation also appeared in the section with different positions of secondary flow and main flow. The transverse variation of dispersion coefficients in a braided channel of the Brahmaputra River was similar to that in the laboratory braided river with a large diversion angle; however, higher values were estimated in the natural braided channel.

ACKNOWLEDGEMENTS

This research was supported by the National Nature Science Foundation of China (Grant Nos 51379058, 51308183, and 51179052), the National Key Technologies R&D Program (2012BAB03B04), and the Major Science and Technology Program for Water Pollution Control and Treatment (Grant No. 2012ZX07103-005).

REFERENCES

Alavian, V. 1986 Dispersion tensor in rotating flows. *Journal of Hydraulic Engineering* **112** (8), 771–777.

Boxall, J. & Guymer, I. 2003 Analysis and prediction of transverse mixing coefficients in natural channels. *Journal of Hydraulic Engineering* **129** (2), 129–139.

Boxall, J. & Guymer, I. 2007 Longitudinal mixing in meandering channels: New experimental data set and verification of a predictive technique. *Water Research* **41** (2), 341–354.

Deng, Z. Q., Singh, V. P. & Bengtsson, L. 2001 Longitudinal dispersion coefficient in straight rivers. *Journal of Hydraulic Engineering* **127** (11), 919–927.

Dow, K. E., Steffler, P. M. & Zhu, D. Z. 2009 Case study: Intermediate field mixing for a bank discharge in a natural river. *Journal of Hydraulic Engineering* **135** (1), 1–12.

Elder, J. 1959 The dispersion of marked fluid in turbulent shear flow. *Journal of Fluid Mechanics* **5** (4), 544–560.

Fischer, H. B. 1978 On the tensor form of the bulk dispersion coefficient in a bounded skewed shear flow. *Journal of Geophysical Research: Oceans* **83** (C5), 2373–2375.

Fischer, H. B., List, E. J., Koh, R. C., Imberger, J. & Brooks, N. H. 1979 *Mixing in Inland and Coastal Waters*. Academic Press, New York.

Fuat Toprak, Z. & Savci, M. E. 2007 Longitudinal dispersion coefficient modeling in natural channels using fuzzy logic. *CLEAN–Soil, Air, Water* **35** (6), 626–637.

Fukuoka, S. & Sayre, W. W. 1973 Longitudinal dispersion in sinuous channels. *Journal of the Hydraulics Division* **99** (1), 195–217.

Holley, E. R. & Abraham, G. 1973 Laboratory studies on transverse mixing in rivers. *Journal of Hydraulic Research* **11** (3), 219–253.

Hou, H. & Christensen, B. 1976 Influence of equivalent sand roughness on the dispersion coefficient in laboratory and natural stream. In: *3rd Annual Symp. Waterways, Harbors and Coastal Engineering Div, ASCE*, Colorado State University, Fort Collins, Rivers, pp. 1179–1198.

Okoye, J. K. 1970 *Characteristics of transverse mixing in open-channel flows*. California Institute of Technology, Pasadena, CA, USA.

Perucca, E., Camporeale, C. & Ridolfi, L. 2009 Estimation of the dispersion coefficient in rivers with riparian vegetation. *Advances in Water Resources* **32** (1), 78–87.

Piasecki, M. & Katopodes, N. D. 1999 Identification of stream dispersion coefficients by adjoint sensitivity method. *Journal of Hydraulic Engineering* **124** (7), 714–724.

Richardson, W., Thorne, C. & Mahmood, S. 1996 *Secondary flow and channel changes around a bar in the Brahmaputra River, Bangladesh*. In: *Coherent Flow Structures in Open Channels* (Ashworth, P. J., Bennett, S. J., Best, J. L. & McLelland, S. J., eds). Wiley, Chichester, UK, pp. 519–543.

Rutherford, J. 1994 *River Mixing*. Wiley Chichester.

Sayre, W. W. & Yeh, T. 1973 *Transverse Mixing Characteristics of the Missouri River Downstream from the Cooper Nuclear Station*, Iowa Inst. of Hydraulic Research, Iowa City, USA.

Schulz, M., Priegnitz, J., Klasmeier, J., Heller, S., Meinecke, S. & Feibicke, M. 2012 Effect of bed surface roughness on longitudinal dispersion in artificial open channels. *Hydrological Processes* **26** (2), 272–280.

Seo, I. W. & Cheong, T. S. 1998 Predicting longitudinal dispersion coefficient in natural streams. *Journal of Hydraulic Engineering* **124** (1), 25–32.

Seo, I. W., Lee, M. E. & Baek, K. O. 2008 2D modeling of heterogeneous dispersion in meandering channels. *Journal of Hydraulic Engineering* **134** (2), 196–204.

Valentine, E. M. & Wood, I. R. 1977 Longitudinal dispersion with dead zones. *Journal of the Hydraulics Division* **103** (9), 975–990.

Webel, G. & Schatzmann, M. 1984 Transverse mixing in open channel flow. *Journal of Hydraulic Engineering* **110** (4), 423–435.

Yotsukura, N., Fischer, H. B. & Sayre, W. W. 1970 *Measurement of Mixing Characteristics of the Missouri River Between Sioux City, Iowa, and Plattsmouth, Nebraska*. Geological Survey Water-Supply Paper. US Geological Survey, Reston, VA, USA.

First received 10 November 2013; accepted in revised form 19 March 2014. Available online 9 May 2014